Joint IRN-FenmTo COPIGAL POLITA Workshop

Generation of fission fragments' spin in microscopic models

Guillaume SCAMPS

Université de Toulouse

L2IT

cnrs

Spin of the fragments

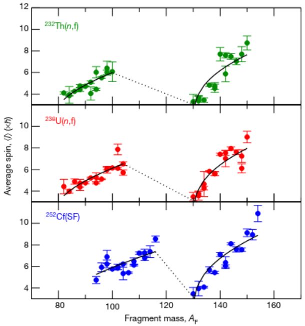

Correlations

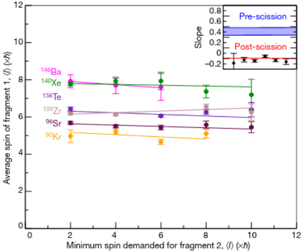

J. N. Wilson, Nature, 590, 566 (2021)

- The average spin follows a sawtooth shape
- No correlations between the spins of the fragments

What generates the fragments' spin ?

Literature

- Thermal excitations
- Quantum fluctuations
- Coulomb force
- Breaking of the neck

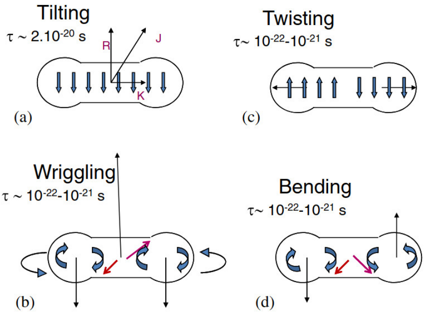

Illustration from B. John, J. Phys., 85, 2, (2015).

Static HFB

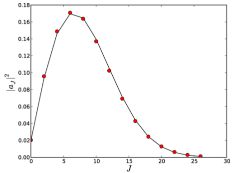

G. F. Bertsch, T. Kawano, and L. M. Robledo, PRC 99, 034603 (2019)

Scission configuration

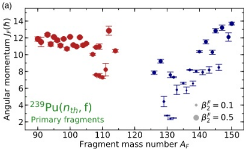

P. Marević, N. Schunck, J. Randrup, and R. Vogt PRC 104, L021601 (2021).

TDHFB - TDSLDA

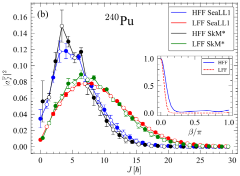

A. Bulgac, et al., PRL 126, 142502 (2021)

Projection method

$$\hat{P}_J \left(|\Psi(J=0)\rangle + |\Psi(J=1)\rangle + \ldots\right) = |\Psi(J)\rangle$$

$$|a_J^F|^2 = \frac{2J+1}{2}\int_0^{2\pi} \sin(\beta)\, P_J(\cos(\beta))\langle\Psi| e^{\frac{-i\hat{J}_x^F\beta}{\hbar}} |\Psi\rangle$$

TDHFB equations

$$i\hbar\frac{\partial}{\partial t}\begin{pmatrix} U \\ V \end{pmatrix} = \begin{pmatrix} h(t) & \Delta(t) \\ -\Delta^*(t) & -h^*(t) \end{pmatrix}\begin{pmatrix} U \\ V \end{pmatrix}$$

TDHFB equations

$$i\hbar\frac{\partial}{\partial t}\begin{pmatrix}U\\V\end{pmatrix}=\begin{pmatrix}h(t) & \Delta(t)\\-\Delta^*(t) & -h^*(t)\end{pmatrix}\begin{pmatrix}U\\V\end{pmatrix}$$

Strengths

- Self-consistent mean field + pairing
- Functional and no other adjustable parameters.
- One-body dissipation
- Large-amplitude collective motion

TDHFB equations

$$i\hbar \frac{\partial}{\partial t} \begin{pmatrix} U \\ V \end{pmatrix} = \begin{pmatrix} h(t) & \Delta(t) \\ -\Delta^*(t) & -h^*(t) \end{pmatrix} \begin{pmatrix} U \\ V \end{pmatrix}$$

Strengths

- Self-consistent mean field + pairing
- Functional and no other adjustable parameters.
- One-body dissipation
- Large-amplitude collective motion

Limitations

- Missing quantum and statistic fluctuations
- Broken symmetries (projection needed)
- Computationally expensive

TDHFB equations

$$i\hbar \frac{\partial}{\partial t} \begin{pmatrix} U \\ V \end{pmatrix} = \begin{pmatrix} h(t) & \Delta(t) \\ -\Delta^*(t) & -h^*(t) \end{pmatrix} \begin{pmatrix} U \\ V \end{pmatrix}$$

TDBCS approximation

Canonical basis evolution :

$$i\hbar\, \dot{\varphi}_\alpha = h\, \varphi_\alpha$$

$$i\hbar\, \dot{n}_\alpha = \kappa_\alpha \Delta^*_\alpha - \kappa^*_\alpha \Delta_\alpha$$

$$i\hbar\, \dot{\kappa}_\alpha = 2\epsilon_\alpha \kappa_\alpha + \Delta_\alpha (2n_\alpha - 1)$$

Strengths

- Self-consistent mean field + pairing
- Functional and no other adjustable parameters.
- One-body dissipation
- Large-amplitude collective motion

Limitations

- Missing quantum and statistic fluctuations
- Broken symmetries (projection needed)
- Computationally expensive

TDHFB framework

- Gogny-TDHFB code
- Gogny D1S interaction
- Hybrid basis :
  - 2D harmonic oscillator (x, y)
  - 1D spatial mesh (z)

Numerical setup

- $\Delta z = 0.8$ fm, $N_z = 52$
- $n_x + n_y \leq N_{\text{shell}} = 9$
- $\hbar\omega = 8$ MeV
- $\Delta t = 2 \times 10^{-3}$ zs

Fissioning nuclei

- ^{230}Th
- ^{240}Pu
- ^{250}Cf

Asymmetric fission region
Heavy fragment influenced by octupole deformation

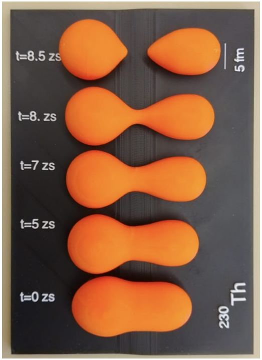

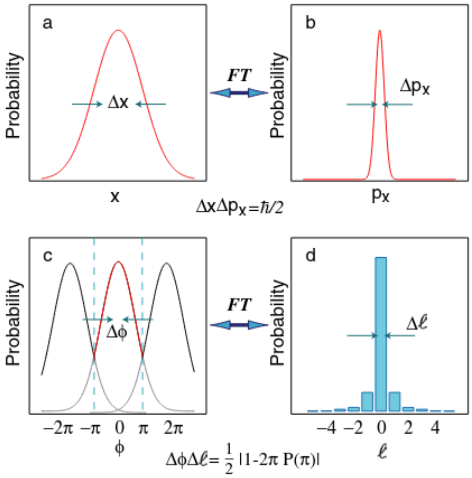

S. Franke-Arnold, et al. New Journal of Physics 6, 103 (2004)

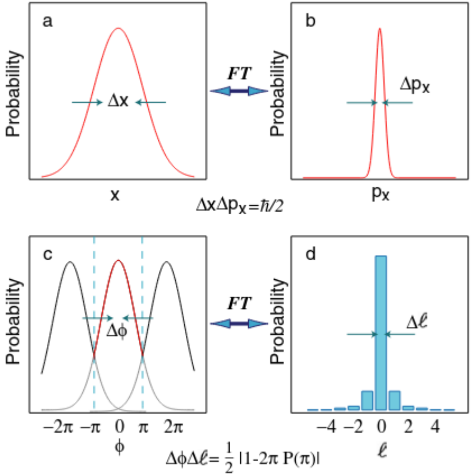

S. Franke-Arnold, et al. New Journal of Physics 6, 103 (2004)

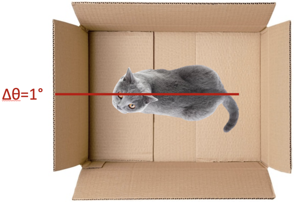

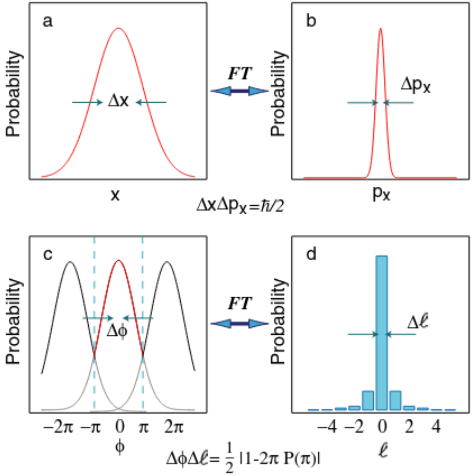

S. Franke-Arnold, et al. New Journal of Physics 6, 103 (2004)

For $\Delta\Theta = 1^\circ$, $\Delta L = 29\hbar$.
For a cat, angular velocity $\omega = 10^{-33}s^{-1}$

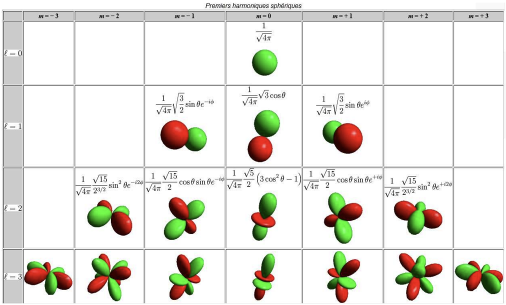

Orientation pumping mechanism

Isotropic potential at scission

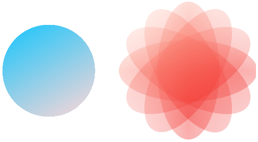

Confining potential at scission

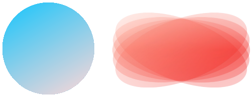

L. Bonneau, P. Quentin, and I. N. Mikhailov, PRC 75, 064313 (2007).

For $\Delta\Theta = 1^\circ$, $\Delta L = 29\hbar$.

For a nucleus, angular velocity $\omega = 10^{20} s^{-1}$

Conceptual difficulty

- Unlike position, angular variables are **periodic**.
- Mean values and fluctuations of an angle are not uniquely defined.
- Restrict to well-oriented wave packet

Orientation–angular momentum uncertainty

$$\Delta\theta\,\Delta L_x > \frac{1}{2}, \qquad (L_x \text{ in units of } \hbar)$$

Analogous relation for L_y.

Gaussian orientation state and spin distribution

Gaussian wave packet :

$$\Psi(\theta,\varphi) = \mathcal{N}\exp\left[-\frac{\theta^2}{4\sigma_\theta^2}\right]$$

Spin cut-off distribution :

$$P(L) = \frac{2L+1}{\mathcal{Z}}\exp\left[-\frac{L(L+1)}{2\sigma_L^2}\right]$$

Heisenberg-type relation :

$$\sigma_\theta\,\sigma_L = \frac{1}{2}$$

Second difficulty : composite nuclei

- In collective Hamiltonian models, angle wave packets are well defined.
- In microscopic approaches, orientation is **not an operator**.
- No direct definition of angular fluctuations.

Proposed approach

- Go beyond the one-body density picture.
- Sample nucleon positions and intrinsic spins from the Bogoliubov vacuum.
- Markov Chain Monte Carlo sampling (`NucleoScope`).
- Determine principal axis event-by-event.

Principal axis determination

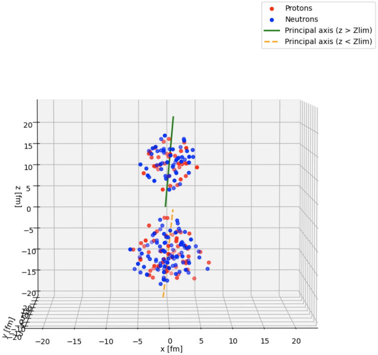

Examples for ^{230}Th.
Red/blue dots : proton/neutron distributions.
Lines : fragment principal axes.

Nucleoscope paper : A. Bernard *et al.*, arXiv :2601.18488 [nucl-th] (2026)

Second difficulty : composite nuclei

- In collective Hamiltonian models, angle wave packets are well defined.
- In microscopic approaches, orientation is **not an operator**.
- No direct definition of angular fluctuations.

Proposed approach

- Go beyond the one-body density picture.
- Sample nucleon positions and intrinsic spins from the Bogoliubov vacuum.
- Markov Chain Monte Carlo sampling (`NucleoScope`).
- Determine principal axis event-by-event.

Principal axis determination

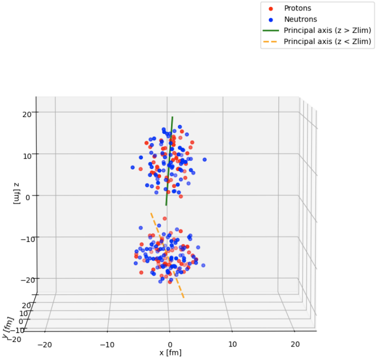

Examples for ^{230}Th.
Red/blue dots : proton/neutron distributions.
Lines : fragment principal axes.

Nucleoscope paper : A. Bernard *et al.*, arXiv :2601.18488 [nucl-th] (2026)

Distribution of θ

- For each sampled event, principal axis of each fragment is computed.
- Obtain θ = angle between fragment axis and global z-axis.
- Construct full probability distribution $P(\theta)$.
- Expectation value $\langle\theta\rangle = 0$ due to symmetry.
- Standard deviation σ_θ characterizes the angular fluctuation.

Physical meaning

- Reflects uncertainty in fragment orientation.
- Geometric definition mainly sensitive to quadrupole deformation.
- Can be used for spin-cutoff estimations.

Angular distribution figure

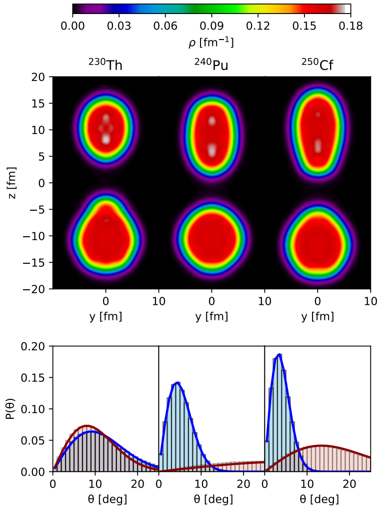

Angular distribution $P(\theta)$ for light (blue) and heavy (red) fragments. Fitted curves illustrate approximate Gaussian behavior.

Angular distribution

$$f(\theta) = \mathcal{N}^2 \sin(\theta) \exp\left[-\frac{\theta^2}{2\sigma_\theta^2}\right]$$

- Excellent agreement with Gaussian form
- Angular fluctuations are Gaussian
- Larger quadrupole deformation $\Rightarrow$ narrower distribution

From σ_θ to spin

$$\sigma_\theta \, \sigma_L = \frac{1}{2}$$

- Extract σ_θ
- Deduce spin cut-off σ_L
- Build spin distribution

Spin distribution

$$P(L) = \frac{2L+1}{\mathcal{Z}} \exp\left[-\frac{L(L+1)}{2\sigma_L^2}\right]$$

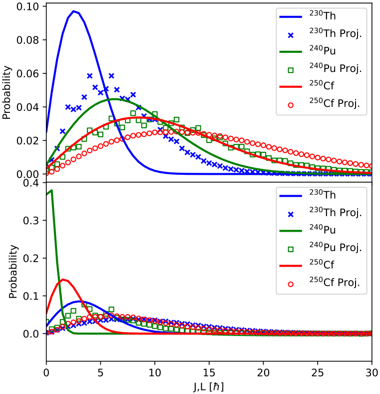

Projection results vs. spin cut-off formula (light : top, heavy : bottom).

Microscopic vs geometric picture

- Exact angular momentum obtained from projection of many-body states.
- Monte Carlo sampling determine the fluctuations of the fragment principal axis from Q_2 deformation.

Octupole deformation

- Principal axis distribution becomes flat.
- Geometric picture underestimates spin.

Spin-cutoff vs deformation

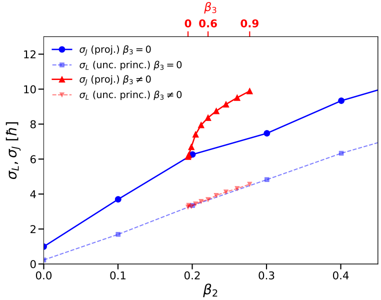

Spin cut-off parameter for ^{144}Ba. Solid lines : projection. Dashed lines : principal-axis uncertainty estimate.

Prolate deformation

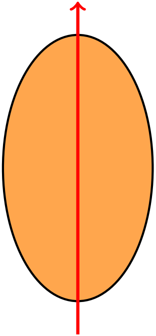

$Q_2 > 0$

Principal axis well defined

Triangular (octupole) configuration

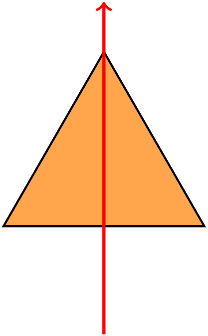

$Q_2 = 0$

Orientation still defined but principal axis isotropic

Uncertainty Relation from Projection

Overlap of rotated many-body states

$$\langle\Psi|e^{i\alpha\hat{J}_z}e^{i\theta\hat{J}_y}e^{i\gamma\hat{J}_z}|\Psi\rangle \simeq \exp\left[-\frac{\theta^2}{8\sigma_\theta^2}\right]$$

- Gaussian approximation for small rotations
- Width σ_θ characterizes angular localization

Physical meaning

- Many-body state localized in rotational space
- Does **not** rely on geometric definition of orientation
- Orientation angle and angular momentum are conjugate variables

Spin fluctuations

Spin cut-off distribution :

$$P(J) = \frac{2J+1}{\mathcal{Z}} \exp\left[-\frac{J(J+1)}{2\sigma_J^2}\right]$$

$$\sigma_\theta\,\sigma_J = \frac{1}{2}$$

Spin Cut-off Parameters from Different Approaches

Nucleus	Frag.	σ_L (uncert. with principal axis)	σ_J (overlap)	σ_J (projection)
^{230}Th	L	2.90	5.74	5.81
	H	3.37	7.84	7.88
^{240}Pu	L	6.79	9.32	9.37
	H	0.75	4.67	4.93
^{250}Cf	L	9.00	12.18	12.27
	H	2.12	6.50	6.63

Key result

- Spin cut-off parameters extracted from :
  - angular fluctuations + uncertainty relation
  - Gaussian overlap fit
  - exact angular-momentum projection
- **Excellent agreement** between overlap and exact projection.
- Error with the principal axis method (miss higher order deformation).

G. Scamps, A. Guilleux, D. Regnier, A. Bernard, Uncertainty Principle and Angular Momentum Generation in Microscopic Fission Models, arXiv :2512.02207 [nucl-th].

Pair breaking mechanism ?

Assuming Cold fission

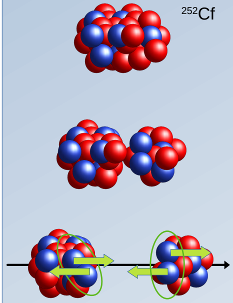

K_H=0 K_L=0

Fully paired fragments
Only even-even fragments

Realistic case

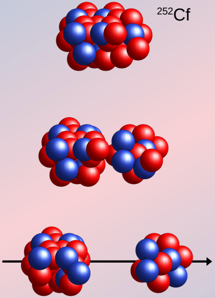

K_H≠0 K_L≠0

Pairs are broken
Every outcome are possible

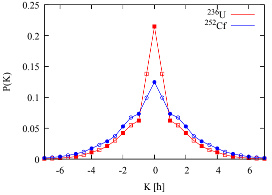

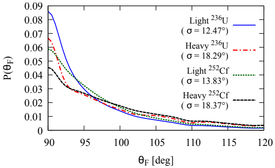

$$\cos\theta_F = \frac{K_F}{\sqrt{S_F(S_F+1)}}$$

G.scamps, I. Abdurrahman, M. Kafker, A. Bulgac, and I. Stetcu, PRC 108 (6), L061602.

^{144}Ba + ^{96}Sr at 16 Fm, Θ_{ini}=25 deg, Functional : Skyrme Sly4d

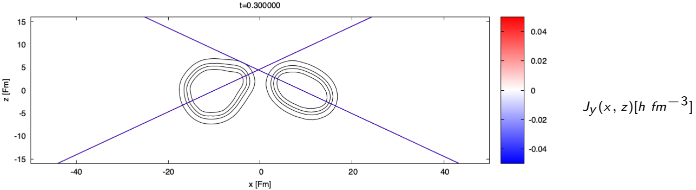

G. Scamps, PRC 106, 054614 (2022).

One body-evolution - One body-observable

^{144}Ba + ^{96}Sr at 16 Fm, Θ_{ini}=25 deg, Functional : Skyrme Sly4d

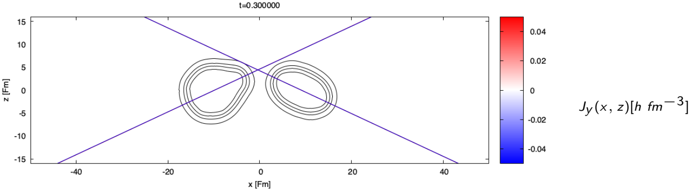

G. Scamps, PRC 106, 054614 (2022).

One body-evolution - One body-observable

^{144}Ba + ^{96}Sr at 16 Fm, Θ_{ini}=25 deg, Functional : Skyrme Sly4d

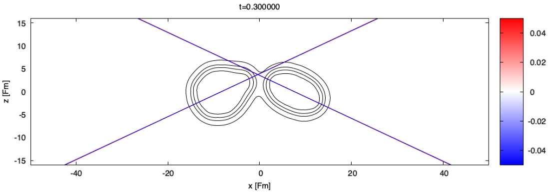

$J_y(x,z)[h\ fm^{-3}]$

G. Scamps, PRC 106, 054614 (2022).

^{144}Ba + ^{96}Sr at 16 Fm, Θ_{ini}=25 deg, Functional : Skyrme Sly4d

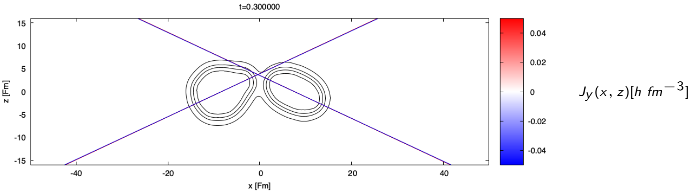

G. Scamps, PRC 106, 054614 (2022).

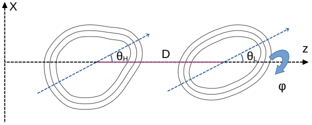

Potential as a function of the light fragment angle

$^{132}Sn + ^{108}Ru$

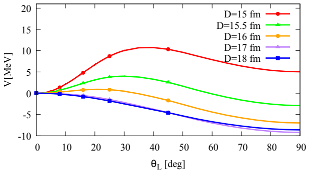

Two torques :

- attractive nucleus-nucleus torque
- repulsive Coulomb torque

Potential as a function of the light fragment angle

$^{144}Ba + ^{96}Sr$. D=15.5 and 20 fm

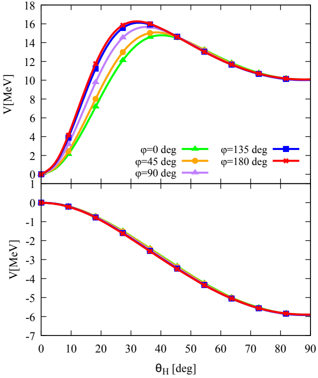

The azimuthal angle doesn't have an important role.

Frozen Hartree-Fock potential

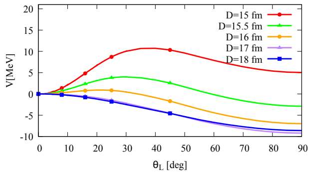

Two torques :

- attractive nucleus-nucleus torque
- repulsive Coulomb torque

4 degrees of freedom

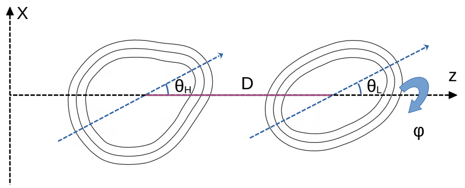

Hamiltonian

$$\hat{H}(D) = \frac{\hbar^2}{2I_H}\hat{L}_H^2 + \frac{\hbar^2}{2I_L}\hat{L}_L^2 + \frac{\hbar^2}{2I_\Lambda(D)}\hat{\Lambda}^2 + \hat{V}(\hat{\Theta}_H, \hat{\Theta}_L, \hat{\varphi}, D)$$

Solved in basis $|L_H, m, L_L, -m\rangle$

G. Scamps, G. Bertsch, Phys. Rev. C 108, 034616(2023).
Similar to the orientation pumping mechanism model Mikhailov, I. N., and Quentin, P. Physics Letters B, 462(1-2), 7-13 (1999)

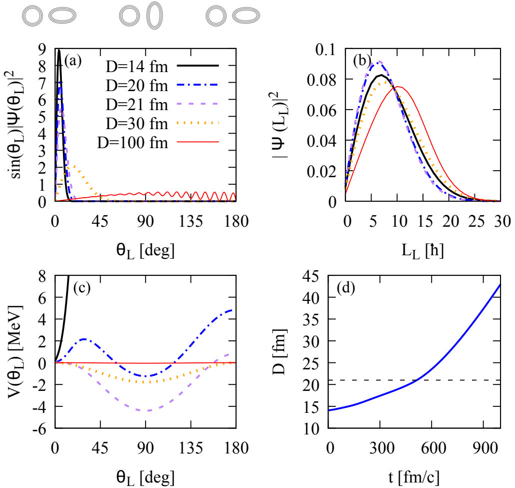

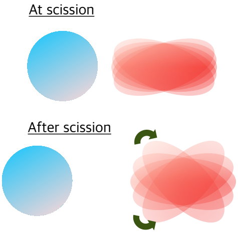

G. Scamps, G. Bertsch, Phys. Rev. C 108, 034616 (2023).

Theoretical tools

- Development of advanced TDDFT approaches with projection techniques and position sampling
- Frozen Hartree-Fock
- Collective Hamiltonian approaches for quantum collective motion

Mechanism for the generation of fragment spin

- Coulomb interaction at scission tends to deform the fragments
- Fragments are oriented along the fission axis
- The uncertainty principle induces angular momentum

Thank you for your attention